Hindawi
Science and Technology of Nuclear Installations
Volume 2020, Article ID 1905019, 12 pages
https://doi.org/10.1155/2020/1905019

Research Article

Experimental Approaches for Manufacturing of Simulated Cladding and Simulated Fuel Rod for Mechanical Decladder

Young-Hwan Kim, Yung-Zun Cho, and Jin-Mok Hur

Korea Atomic Energy Research Institute, Daedeok-daero 989-111, Yuseong-gu, Daejeon 305-353, Republic of Korea

Correspondence should be addressed to Young-Hwan Kim; yhkim3@kaeri.re.kr

Received 30 August 2019; Revised 13 December 2019; Accepted 20 December 2019; Published 24 January 2020

Academic Editor: Arkady Serikov

We are developing a practical-scale mechanical decladder that can slit nuclear spent fuel rod-cuts (hulls + pellets) on the order of several tens of kgf of heavy metal/batch to supply UO_2 pellets to a voloxidation process. The mechanical decladder is used for separating and recovering nuclear fuel material from the cladding tube by horizontally slitting the cladding tube of a fuel rod. The Korea Atomic Energy Research Institute (KAERI) is improving the performance of the mechanical decladder to increase the recovery rate of pellets from spent fuel rods. However, because actual nuclear spent fuel is dangerously toxic, we need to develop simulated spent fuel rods for continuous experiments with mechanical decladders. We describe procedures to develop both simulated cladding tubes and simulated fuel rod (with physical properties similar to those of spent nuclear fuel). Performance tests were carried out to evaluate the decladding ability of the mechanical decladder using two types of simulated fuel (simulated tube + brass pellets and zircaloy-4 tube + simulated ceramic fuel rod). The simulated tube was developed for analyzing the slitting characteristics of the cross section of the spent fuel cladding tube. Simulated ceramic fuel rod (with mechanical properties similar to the pellets of actual PWR spent fuel) was produced to ensure that the mechanical decladder could slit real PWR spent fuel. We used castable powder pellets that simulate the compressive stress of the real spent UO_2 pellet. The production criteria for simulated pellets with compressive stresses similar to those of actual spent fuel were determined, and the castables were inserted into zircaloy-4 tubes and sintered to produce the simulated fuel rod. To investigate the slitting characteristics of the simulated ceramic fuel rod, a verification experiment was performed using a mechanical decladder.

1. Introduction

Spent fuel, which is an essential by-product of electricity generation by nuclear power reactors, is highly radioactive. However, it could be a valuable asset if it is effectively recycled. With the increase in the cumulative amount of spent fuel in Korea, the development of methods for reliable and effective management of this spent fuel has become an important KAERI (Korea Atomic Energy Research Institute) mission. With such a background, KAERI is developing mechanical head-end process for pyroprocessing [1, 2]. Mechanical head-end processing of SF disassembly, extraction of rods, shearing of the extracted rods, and mechanical decladding shall be performed in advance as the head-end process of the pyroelectro-reduction process [3, 4]. In the shearing of the extracted rods, generally, the characteristics of the shearing method in the head-end process is different according to the wet method or dry method. Especially, the pyroprocess, which is a dry process, shall have the efficient shearing method connected to the postprocess of the mechanical head-end process in advance. The mechanical decladder is required to shear the SF rods generated from the nuclear plant for rod-cuts (cladding tube + pellets), and tools such as saw, wire, and punch and die are used widely for SF rods' shearing or cutting in the air or in the water inside the hot cell. Also, the original form of the cross section of the rods after the shearing should be nicely maintained because the rod-cut cannot be used for the mechanical decladding if the circular section of the cladding is deformed during shearing or cutting. In addition, for oxidation processing of the spent fuel in the head-end process, a mechanical decladding

device for decladding rod-cuts is necessary. The mechanical decladder is an apparatus for separating and recovering fuel material and cladding tubes by horizontally slitting the cladding tube of a fuel rod and a defective irradiated fuel rod [5]. Furthermore, for recycling the spent nuclear fuel, recovery of fuel materials in the cladding tube is very important [6]. For this, a mechanical decladding method and an oxidative decladding method may be commonly used [7, 8]. However, unlike other countries, KAERI has only developed a longitudinal slitter concept for preliminary testing by using the simulated fuel [3, 4], also, a mechanical decladder that can handle several tens of kgf HM/batch is developed to supply UO_2 fragments to a voloxidation process [9, 10]. In the mechanical decladding method, decladding cylindrical nuclear fuel by rolling-straightener technique has been investigated at the Egypt Atomic Energy Establishment. Decladding by rolling-straightener technique is based on expected deformation in clad leading to adequate loosening of cladded fuel material and in principle on helical rolling of a tube in close contact with a mandril [8]. The method could be widely applied for nuclear fuel cladded with various materials such as aluminium, stainless steel, zircaloy-2 and zircaloy-4, and inconel-702. However, this method differs from KAERI's decladding in the material recovery method in fuel rods. Also, in the oxidative decladding method, a horizontal voloxidizer with 2 kgHM/batch capacity was studied at the Japan Atomic Energy Research Institute (JAERI) by using the simulated rod-cuts, and UO_2 pellets containing 750 ppm Li_2O was supplied from Mitsubishi Metal Industries Inc. and used as a simulated spent fuel. This fuel was slightly irradiated in the JAERI research reactor. However, rod-cuts for oxidative decladding cannot be used for mechanical slitting because of the different decladding methods.

KAERI is improving the performance of mechanical decladders to increase the recovery rate of pellets from spent fuel rods [11]. However, a test to determine the decladding performance of the mechanical decladder was conducted using the simulated tube and sintered simulated ceramic fuel rod (castable + Zry-4 tube), respectively, instead of spent fuel because we have not received a joint determination yet. Also, as the actual nuclear spent fuel has dangerous toxicity, it cannot be used directly to improve the performance of a mechanical decladder. Therefore, it is necessary to develop simulated spent fuel rods to develop various decladding technologies for recycling spent fuel and for continuous experiments using mechanical decladder. In this paper, we address procedures to develop a simulated cladding tube and simulated fuel rod with physical properties similar to those of spent nuclear fuel. Also, decladding condition and possible temperature and slitting force were also investigated through the verification of mechanical decladding. In addition, this paper presents the fabrication conditions of simulated tube and fuel rod that will be used for a mechanical decladder test and enhancement. However, the design conditions of the simulated rod-cuts (cladding tube + pellets) to be used during the mechanical decladding process were not determined in this study. In the future, the simulation pellet design requirements for the production of enhanced spent fuel rod-cuts (simulation tubes + simulation pellets) should be studied.

2. Experimental Methods

2.1. Mechanical Decladder. Figure 1 gives a view of the practical-scale mechanical decladder. The entire configuration consists of an autofeeding basket module that continuously feeds rod-cuts, a hydraulic cylinder module, a power unit module, and a loading unit module, which sets and presses rod-cuts. Additionally, it includes a blade module that separates a rod-cut advanced by the extrusion pin into a hull piece and a pellet piece, a blade module housing that can be rotated alternately using four blade modules, a hulls and pellets basket module, another feeding system module, a control panel module, and a supporter module [12].

In a mechanical decladder, a decladding assembly as a unit for rod-cuts includes slitting blades for decladding and rollers for guiding the extrusion of cladding tubes [13]. The slitting intervals of rod-cuts with different diameters are controlled by adding or removing a spacing plate between a slitting blade and a ranch bolt for fixing the slitting blade to the slitting assembly. The slitting portion is placed at the end of the rollers, and the distance between a guide bar and a blade roller in the roller fixing portion is reduced in the direction toward the slitting portion. The decladding of rod-cuts is performed by the rotation of three circular cutting blades inserted among the rollers arranged at 120° intervals. The rollers receive and transfer fuel rods into the entrance by using the extrusion pin. The side-view schematic of the 3-CUT blade module is shown with the housing removed to illustrate the configuration of the module (Figure 2). Each row of slitting blades is indexed from the center of the assembly to progressively cut into tubing. Upon exiting a rod-cut, hulls and pellets are collected directly below the assembly [12].

2.2. Methods. Performance tests of the mechanical decladder were performed to evaluate its decladding ability with two types of simulated rod-cuts (simulated tube + brass pellets and zircaloy-4 tube + simulated ceramic fuel rod) as shown in Figure 3. In order to fabricate the simulated spent fuel rod-cuts (simulated tube + simulated pellets), it is necessary to have decladding requirements such as slitting characteristics of spent fuel cladding and compression stress of pellets. This paper aims to produce design requirements for the simulated spent fuel rod-cuts with similar slitting requirements to spent fuel. For this purpose, the slitting characteristics of the simulated spent fuel cladding were examined, and the compressive stress of the simulated spent fuel rod that was able to slit the spent nuclear fuel was derived.

In the first step, a simulated tube was developed for analyzing the slitting characteristics of the cross section of the spent fuel cladding tube. For this, an apparatus for the

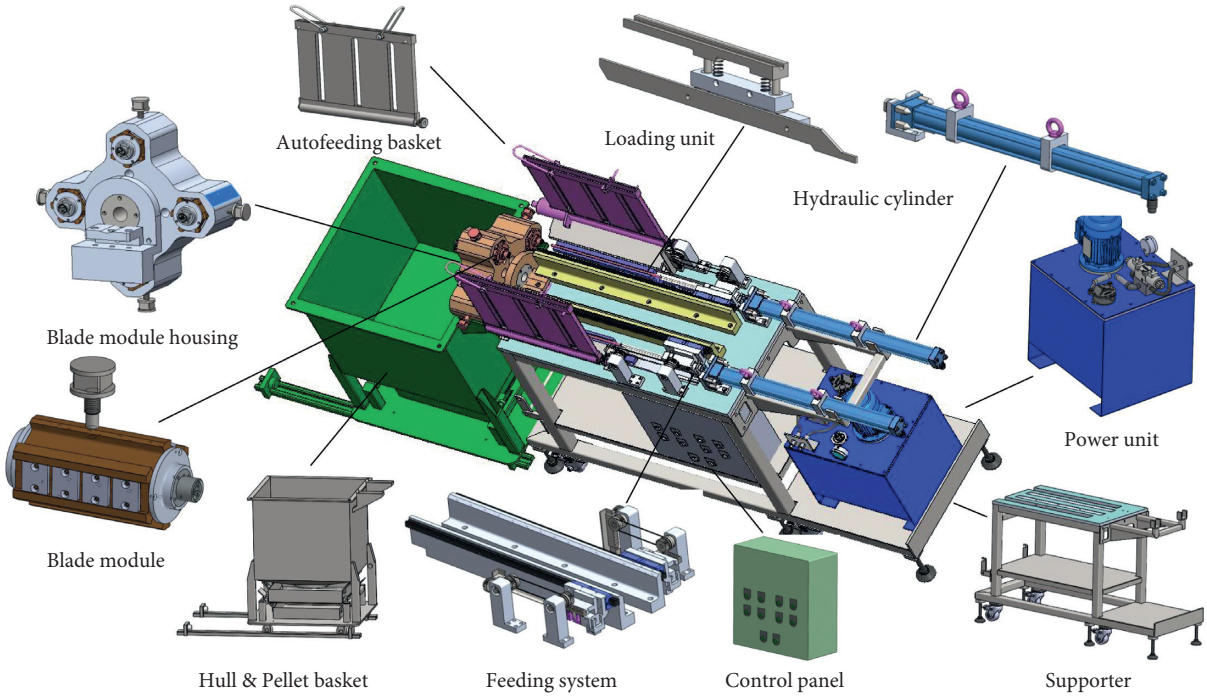

Figure 1: Practical-scale mechanical decladder.

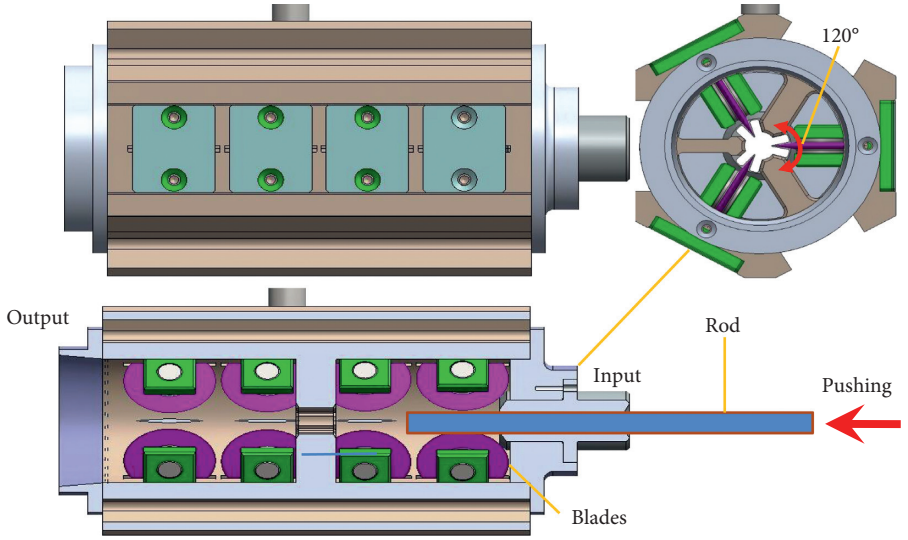

Figure 2: Schematic of 3-CUT blade module.

simulated cladding tube (autoclave furnace) was made to fabricate a simulated cladding tube with mechanical properties similar to those of an actual nuclear spent fuel cladding tube. Commercialized zircaloy tubes were put into an autoclave furnace and the preliminary cladding tubes were manufactured at different temperatures (300, 400, 500, 600, and 700°C). Mechanical material properties such as tensile strength (YS, MPa), yield strength (UTS, MPa), and elongation (EL, %) were analyzed using a universal testing machine after the preliminary simulation cladding tube was manufactured. Using the results of the analysis, a simulated cladding tube similar to the real PWR spent fuel cladding was selected from the preliminary cladding tubes, and these were fabricated for the mechanical decladding test. After slitting, the decladded specimens of the simulated hull were analyzed and evaluated for durability (abrasion and brittleness) of the fractured blade surfaces using a SEM (scanning electron microscope). The simulated ceramic fuel rod with mechanical properties similar to the pellets of actual PWR spent fuel were produced for checking whether the mechanical decladder could slit the real PWR spent fuel. In decladding of the simulated ceramic fuel rod with the mechanical method, one of the important characteristics of the pellet is compressive stress.

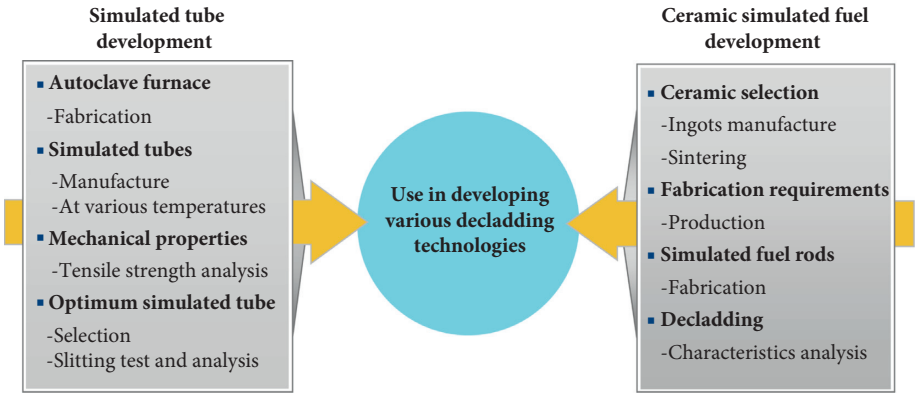

Figure 3: Manufacturing considerations of simulated cladding and simulated fuel.

The compressive stress of the PWR spent UO_2 pellet with average burnup of 55 GWd/tU is approximately 120–130 MPa [14]. In this test, castable powders were used to simulate the compressive stress of the real spent UO_2 pellet. To produce the manufacturing requirements of the simulated ceramic fuel rod, castable, water, and shale were mixed, and various ceramic ingots were prepared according to shale size and mixing time. In addition, green ceramic ingots were sintered at temperatures (800, 1100, 1400, and 1700°C) using a tubular furnace with argon atmosphere and the compressive stresses of the sintered ingots were analyzed. The requirements for the production of simulated pellets with compressive stresses similar to those of actual spent fuel were derived based on the analysis results. Castables were inserted into the zircaloy-4 tubes and sintered to produce the simulated fuel rods. To investigate the slitting characteristics of the simulated ceramic fuel rod similar to that of spent fuel rod, a verification experiment on the simulated ceramic fuel rod was performed using a mechanical decladder.

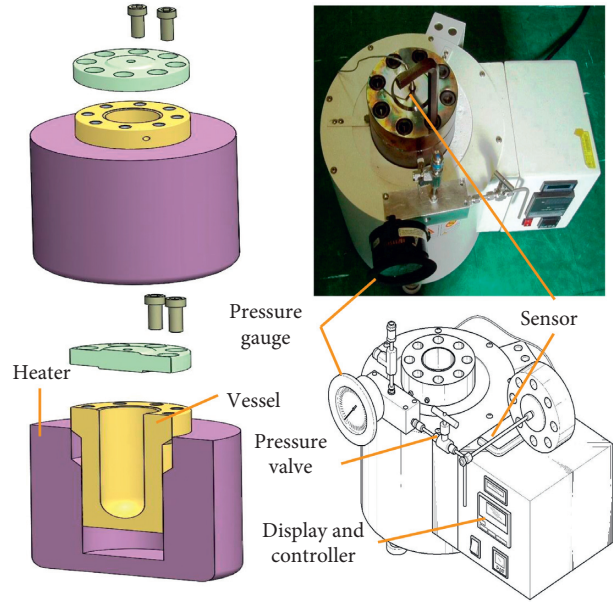

Figure 4: Simulated tube manufacturing apparatus.

3. Simulated Cladding Tube Manufacture

3.1. Autoclave Furnace Fabrication. A zircaloy-4 tube was used to fabricate the simulated cladding tube, and a simulated cladding tube manufacturing machine (autoclave furnace: length 185, height 600, and width 150 mm) was constructed as shown in Figure 4. The main components of the autoclave furnace are heater, control system, vessel, internal pressure gauge, and temperature sensor. Continuous heating of the autoclave furnace with water in the vessel causes the internal pressure of the furnace to rise excessively. To prevent this, a pressure gauge and a regulating valve were constructed, and a temperature control gauge was attached to prevent it from rising above a certain temperature. The specifications of these major components are shown in Table 1. A commercially available actual zircaloy-4 tube (PWR 16 × 16, length 500 mm, outer diameter: 9.5 mm, inner diameter 8.36 in) was used to make a simulated cladding having similar values to the mechanical properties of the spent nuclear fuel. After obtaining the optimal conditions, 20 simulated cladding tubes were prepared for the test.

Table 1: Specifications of autoclave furnace.

Feature	Standard	Remarks
Device pressure	0–100 kgf	Maximum pressure
Furnace heating temperature	700°C (Max.)	Maximum temperature
Voltage	220 V	
Phase	One phase	
Power	3.5 kW	
Current	35 A	
Pressure gauge	Pressure valve control	With 1
Thermometer	Temperature control	With 1

3.2. Simulated Cladding Tube Tensile Test. The simulated cladding tube was manufactured as follows. The control unit raises the temperature (300, 400, 600, and 700°C) and evaporates the water to maintain the internal pressure of the autoclave at 110 bar for 20 h while heating. The temperature-dependent simulated cladding tube was fabricated

as shown in Figures 5(a) and 5(b). To know the mechanical properties (tensile strength, yield strength, elongation, etc.), we performed a tensile test of the simulated cladding using a universal testing machine as shown in Figure 5(c) [15].

3.3. Simulated Cladding Tube-Rod Slitting. The simulation rod-cuts were made by inserting brass pellets into 20 commercial zircaloy tubes using the autoclave furnace at optimum manufacturing conditions (120 ml water, temperature 500°C, and internal pressure 110 bar, maintained for 20 h). Brass pellets were used for decladding because the compressive stress of the brass pellets is higher than that of real PWR spent UO_2 pellets. If there is less reaction force against pellet in the tube, the mechanical decladder cannot slit the tube-rod, so we used brass pellets instead of the real spent fuel pellets. For the mechanical decladding, the simulated rod-cut is filled with 50 brass pellets (Ø $9.5 \times L$ 10 mm) in a Zry-4 tube (OD $10.7 \times L$ 500 mm) as shown in Figure 6(a). We performed a mechanical decladding test using the simulated tube-rods to analyze the slitting characteristics as shown in Figure 6(b). The fracture surfaces (Figures 6(c) and 6(d)) of the decladded hull specimens and the blades used for slitting were analyzed by SEM, and the durability of the blades (abrasion, damage, etc.) was evaluated.

4. Simulated Ceramic Fuel Rod Manufacture

4.1. Ceramic Simulated Ingot Preparation. To simulate the compressive stress of spent nuclear fuel, we conducted the experiment according to the size of the shale and the mixing time using castable (Al_2O_3-95% + CaO-5%). We derived the sintering temperature for producing the simulated fuel. The ceramic simulated ingots were prepared by mixing castable powders and shale stone with 5 wt% of water followed by filling the slurry into the mold, vibrating, drying at 200°C for 12 h, and then sintering at 800, 1100, 1400, and 1700°C for 25 h in a tubular furnace. As shown in the Figures 7(a) and 7(b), the castable ceramics and shales (shale size: none, 1, 3, and 4 mm) were mixed with a mixer (for 5, 10, and 15 minutes). The castable ingots of 167 mm × 40 mm × 40 mm (length × width × height) were fabricated as shown in Figures 7(c) and 7(d). After manufacturing, the castable ingots were sintered up to 1700°C and analyzed.

4.2. Simulated Ceramic Fuel Rod Slitting. The decladding performance test of the mechanical decladder was carried out using the sintered simulated ceramic fuel rod (castable + Zry-4 tube). In the decladding test, 6 pieces of the sintered simulated ceramic fuel rod were loaded in an automatic feeding basket and slit by utilizing the 3-CUT blade modules in the housing. The hulls and simulated pellets were collected in a collection container. The decladding force and slitting velocity of the sintered simulated ceramic fuel rods were measured by using the load cell and a data acquisition system.

5. Results and Discussion

5.1. Simulated Cladding Tube Axial Tensile Stress. Tensile tests were carried out on five simulated cladding tubes made at different temperatures to find values similar to actual spent fuel cladding. In Figure 8, the axial tension stresses of the simulated fuel rods did not fall after 13% of strain because the contact time on the temperature in the furnace are shorter than those of spent fuel in the nuclear reactor, resulting in high ductility. On the other hand, the curve of the axial tension of spent fuel is sharply reduced because spent fuel stays in the reactor for a long time, reducing the ductility of the material and increasing brittleness. However, the ultimate yield stress point is more important than the yield point for mechanical decladding. Therefore, the tube with the most similar ultimate yield stress point to the spent fuel tube is the zircaloy-4 tube at 500°C. As a result of the test, the simulated cladding tube with values most similar to the actual spent fuel cladding tube is the No. 3 zircaloy-4 tube as shown in Figure 8 and Table 2. Table 3 shows the axial tensile test results for the spent fuel cladding, the zircaloy cladding, and the simulated cladding tube. According to R. S. Daum, the mechanical properties of the investigated zircaloy-4 were reported (tensile strength 578 MPa, yield strength 706 MPa, and elongation 7%) [16]. On these bases and Table 3, we see that the mechanical properties of the actual spent fuel and the simulated cladding tube are similar [17–19]. On the order hand, existing mechanical property databases for zircaloy-4 include data from biaxial tube burst, axial tensile, and ring tensile tests for cladding irradiated up to about 60 GWd/MTU [20, 21]. However, the database for cladding irradiated to high fuel burnup is not extensive with regard to temperature and strain rates. Also, most of the tensile data are in the axial direction and the quality of the ring tensile data is suspect [16]. Therefore, it is essential to improve the quality of database to include accurate axial tensile properties and to broaden the investigation of highly degraded cladding, taking into account the combined effects of oxidation, corrosion, and radiation damage if the blade has been used for a long time.

5.2. Simulated Cladding Tube Properties. The conditions and fracture surfaces of the hulls were observed after decladding. Figure 9 shows the fracture surface of the zircaloy-4 tube and simulated cladding tube after decladding. The SEM was used to observe the fracture surface of hull, and the fracture surface was analyzed at 1000 times' magnification. From the SEM image, it is observed that the fracture surface of the simulated cladding tube is rougher than the fracture surface of the fresh zircaloy-4 cladding tube, and that the simulated cladding tube has higher hardness and brittleness than the fresh zircaloy-4 cladding tube due to some debris [22].

As shown in Figures 10(a) and 10(b), the durability of blade abrasion after decladding test using 20 zircaloy cladding tubes and simulated cladding tubes, respectively, was investigated on the blade surface using a SEM. In addition, as shown in Figure 10(c), the slitting forces on the

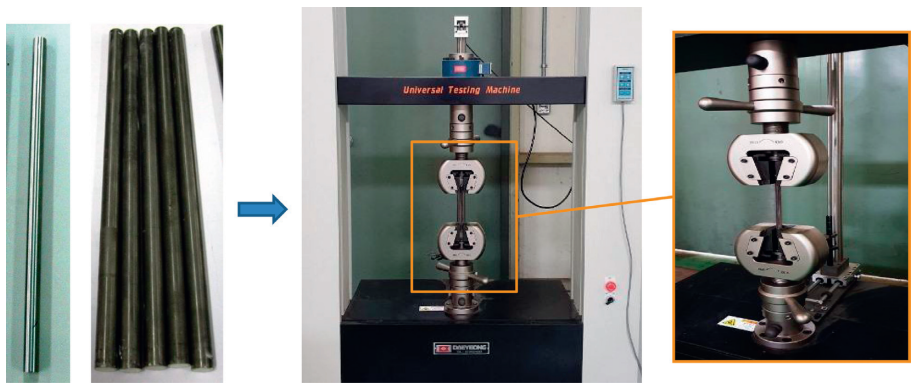

Figure 5: Tensile test of cladding: (a) fresh zircaloy, (b) simulated tube, and (c) universal testing machine.

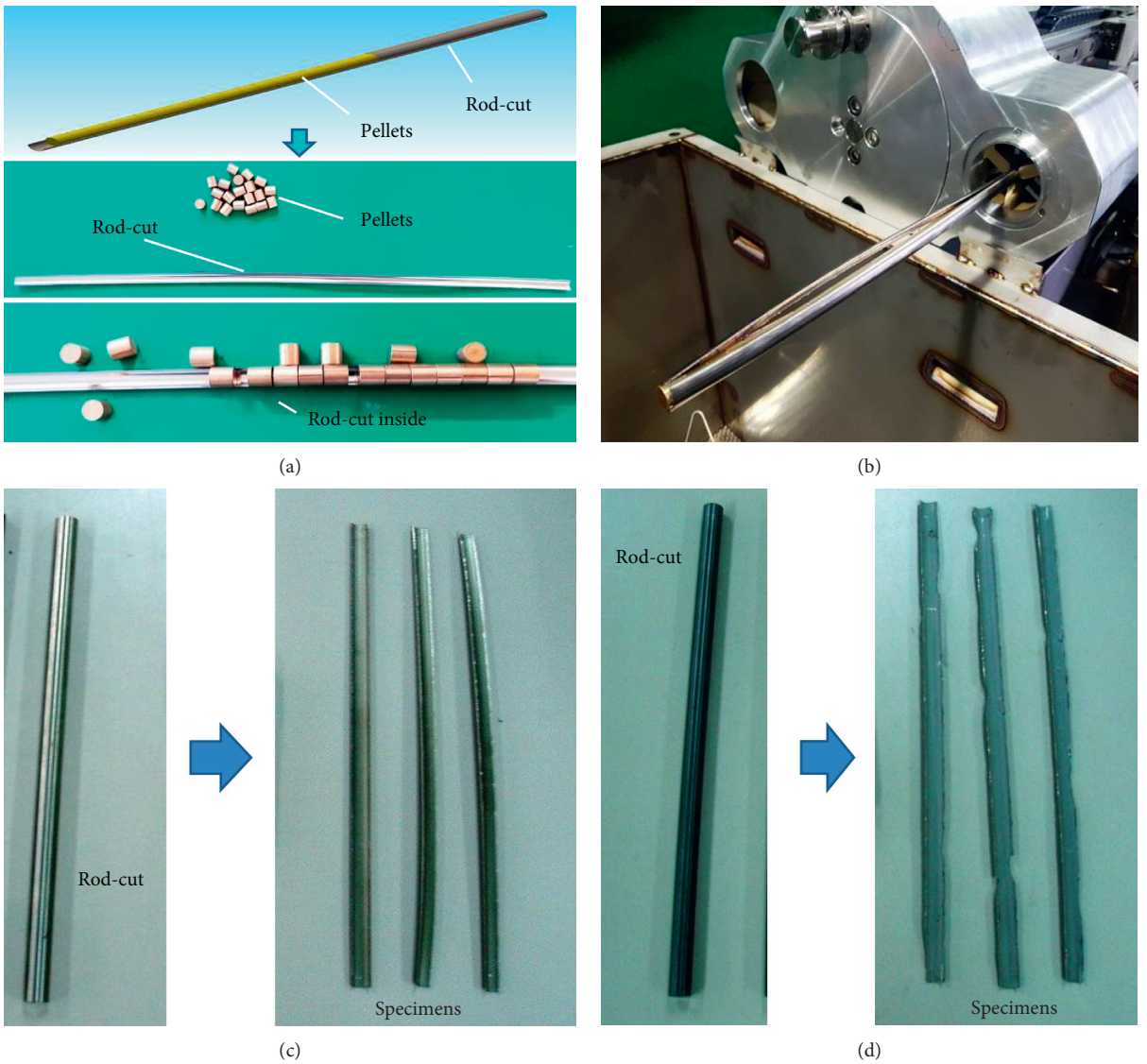

Figure 6: Decladding test of zircaloy tube and simulated cladding tube: (a) rod-cut, (b) decladding test, (c) fresh Zry-4 rod-cut specimens, and (d) simulated rod-cut specimens.

Figure 7: Fabrication of castable ingots: (a) stone selection, (b) mixing, (c) before sintering, and (d) after sintering.

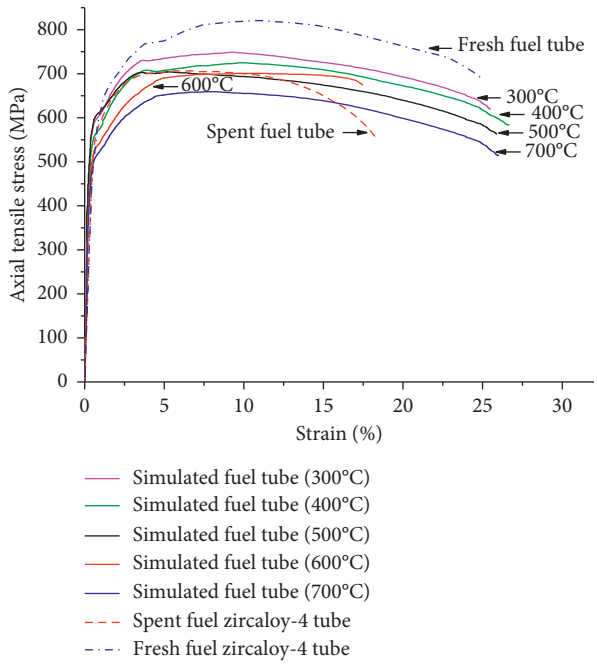

Figure 8: Axial tensile stress of simulated cladding tubes.

cladding tube were measured using a load cell and RSC232 during decladding of the zircaloy and the simulated cladding tube. The blade observation reveals that the decladded blades of the simulated cladding tube has less durability (abrasion) than the decladded blades of the fresh zircaloy-4 cladding tube as shown in Figure 10. In addition, because of the decladding of the rod-cuts, the slitting force of the fresh cladding tube averaged 380 kgf and that of the simulated cladding tube averaged 281 kgf.

5.3. Simulated Ceramic Fuel Rod Compressive Stress. The compressive strength changed depending on the sintering temperature. It was obtained by the destructive testing method presented in Figure 11. The compressive strength was the highest when the size of the shale that could enter the zircaloy tube diameter (ID Ø 9.5 mm) was 4 mm as shown in Figure 11. To determine the optimum sintering temperature, 4 mm shales and castable were mixed according to the mixing time (5, 10, and 15 min) and castable ingots were manufactured. After fabrication, the castable ingots were sintered up to 1700°C and analyzed. As shown in Figure 12, after 13 h of drying at 200°C and sintering up to 1700°C for 25 h, the castable ingots show remarkable high values of initial mechanical characteristics due to the formation of a hydraulic bond in the CaO (cement) in the castable (98% Al_2O_3 and 2% CaO). The castable ingots that were treated at 800, 1100, 1400, and 1700°C for 37 h show significantly improved strength due to CaO. This is caused by the interdiffusion of atoms and ions among the components, with the aim to develop an energetically stable structure and

Table 2: Axial tensile test of simulated tubes.

Simulated tubes	Conditions			Results		
	Temp. (C)	Pressure (bar)	Retention time (h)	YS (MPa)	UTS (MPa)	EL (%)
Zircaloy-4 no. 1	300	110	20	598	748	9
Zircaloy-4 no. 2	400	110	20	571	724	9
Zircaloy-4 no. 3	500	110	20	583	702	9
Zircaloy-4 no. 4	600	110	20	532	700	9
Zircaloy-4 no. 5	700	110	20	520	659	9

Table 3: Axial tensile test of spent fuel, fresh zircaloy-4, and simulated cladding.

Tubes	Tensile stress & strain			
	YS (MPa)	UTS (MPa)	EL (%)	Temp. (°C)
Fresh zircaloy-4	691	820	20	Room
Spent fuel	578	706	7	350
Simulated	583	702	9	500

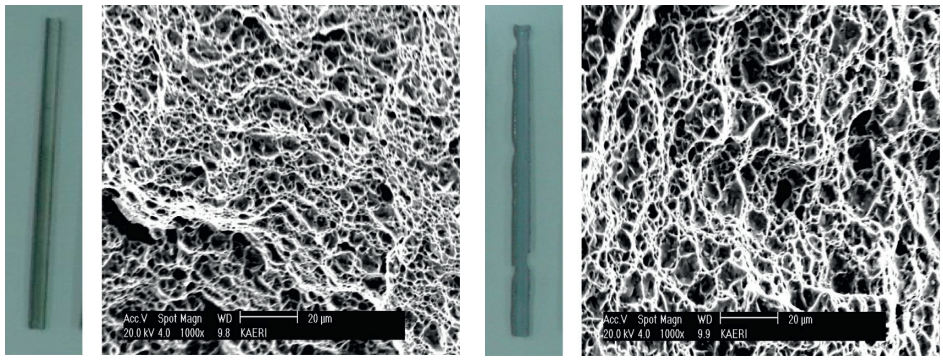

(a) (b)

Figure 9: Hull fracture surface after decladding: (a) fresh Zry-4 and (b) simulated.

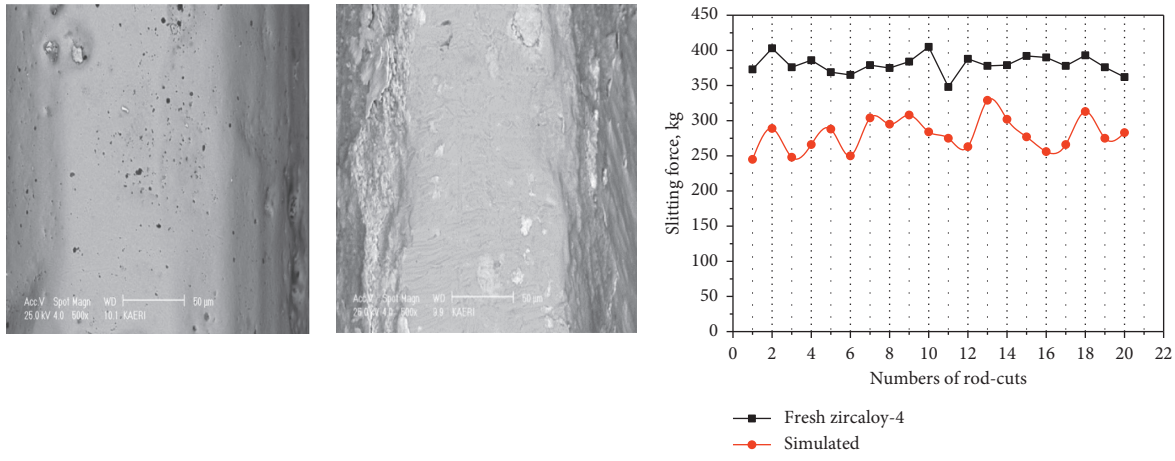

(a) (b) (c)

Figure 10: Abrasion blade edge (SEM: 500x) and slitting force after decladding: (a) fresh Zry-4, (b) simulated, and (c) slitting force.

therefore better mechanical properties. It is obvious that the castable ingots sintered at 1100 and 1400°C for 37 h achieved 70% and 90% of the compressive strength, respectively, of the castable ingots that were treated at room temperature. Similar results and trends can be noticed for the flexural strength values depending on the sintering temperature as shown in Figure 12. The compressive strengths of the castable ingots that were sintered at 1700°C are very high,

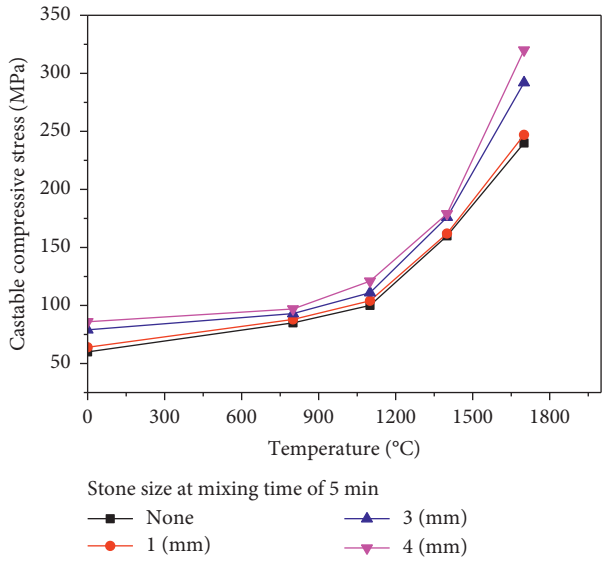

Figure 11: Castable ingot compressive stresses according to stone size.

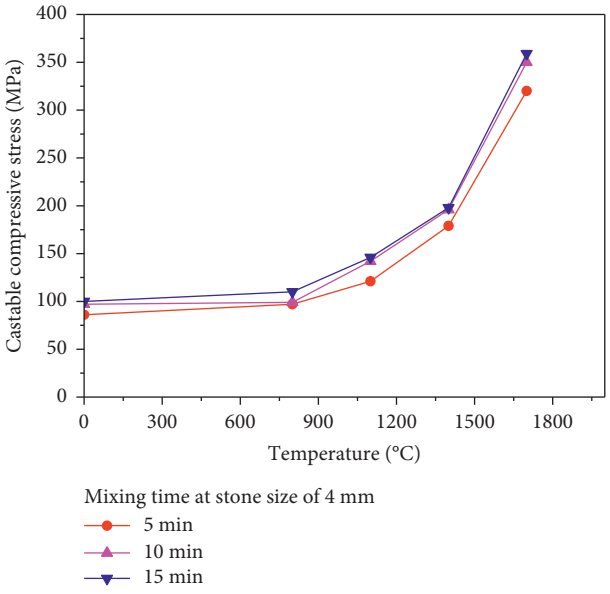

Figure 12: Castable ingot compressive stress according to mixing time.

reaching an almost 260% increase over the reference castable ingots (dried at 200°C) due to more sintering. Considering the above results, the compressive stress (126 MPa) of the castable ingots could be maintained when the mixing time was 10 minutes at 900°C. Therefore, the sintering temperature of the simulated pellet was determined to be 900°C so that the simulated pellet has a strength similar to the compressive stress (120–130 MPa) of the spent nuclear fuel (Figure 12).

Figure 13 shows the compressive stress value of the ceramic simulated rod-cuts. The compressive stress value increased to approximately 126 MPa after the sintering process at 900°C. The compressive stress of the sintered

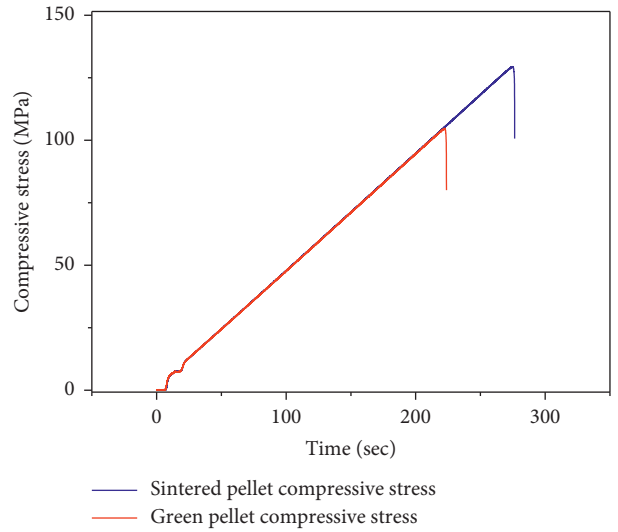

Figure 13: Compressive stress of ceramic simulated ingot.

pellets was increased by 24 MPa than the green pellets, which is the reason why the heated particles were hardened in close contact with each other through thermal activation process while the particles of the ceramic pellets were heated at a temperature below the melting point. Table 4 shows the requirements for producing a simulated nuclear fuel that is similar to spent nuclear fuel.

5.4. Simulated Ceramic Fuel Rod Manufacture. Simulated ceramic fuel rods having compressive stress values similar to those of real UO_2 pellets (120–130 MPa) were prepared by mixing castable powders and 10 vol% of shale stone with 5 wt% of water. The slurry was filled into a Zry-4 tube (ID 9.45 × OD 10.75 × L 500 mm), vibrated, and dried at 200°C for 12 h and then sintered at 900°C for 25 h in a tubular furnace with argon gas as shown in Figures 14(a), 14(b), and 14(c) [14, 23].

5.5. Simulated Ceramic Fuel Rod Slitting. Due to the lack of the reaction force of the simulated pellet, the simulated ceramic fuel rod that was sintered at 800°C and 92 MPa (compressive stress) was split on one side only (Figure 15(a)). However, the simulated ceramic fuel rod that was sintered at 900°C was split into three pieces by the mechanical decladder as shown in Figure 15(b). The average decladding (or slitting) force was approximately 235 kgf as shown in Figure 15(c) [24]. This leads us to estimate that the mechanical decladder can be used for decladding of the PWR spent fuel rod-cut, which has a length of 500 mm. However according to Lee [3], based on the average fuel rod burnups, fuel rods with an average burnup of up to 52.3 GWd/tU showed above 99%, but higher burnup fuels of above 54.9 GWd/tU were below 97.52% in the decladding efficiency. It was interpreted that variations in decladding efficiency with fuel burnups were closely linked to the opening characteristics of the gap between the pellets and cladding.

Table 4: Fabrication requirements of the simulated ceramic fuel rod.

Contents	Fabrication requirements	Remark
Ceramic material	Castable powders	98% Al_2O_3, 2% CaO
Water	5 wt%	
Shale stone	10 vol%	
Shale size	4 mm or less	
Mixing time	10 min	At room temperature

(a) (b) (c)

Figure 14: Preparation of ceramic (castable) rod-cuts: (a) fabrication, (b) tubular furnace, and (c) sintering.

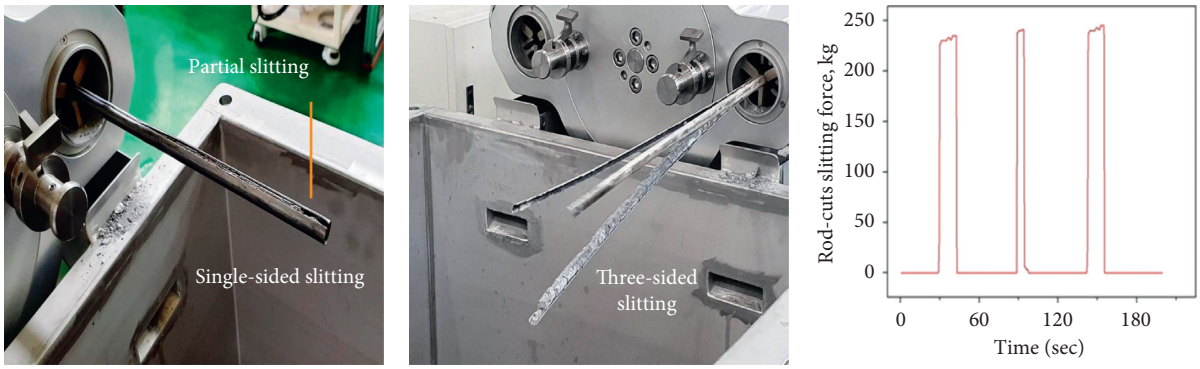

(a) (b) (c)

Figure 15: Decladding of simulated ceramic fuel rod with mechanical decladder: (a) decladding (sintered at 800°C), (b) decladding (sintered at 900°C), and (c) decladding force.

6. Conclusions

Mechanical tests (tensile stress) of simulated cladding tubes allow us to produce a simulated cladding tube having mechanical properties similar to those of actual spent fuel tubes. We can then use it to improve the performance of the mechanical decladder. In this study, a commercial zircaloy cladding tube was introduced in the autoclave furnace under optimum conditions (120 ml water, temperature 500°C, internal pressure 110 bar, and maintained for 20 h). The measured characteristics are similar to those of the actual spent fuel tube (tensile strength 578 MPa, yield strength 706 MPa, and elongation 7%). Thus, the decladding tests were carried out with these. SEM analyzes of the cladding tube specimens were performed to evaluate the decladding characteristics of the spent fuel. We found that the decladding force of the simulated cladding tube (tensile strength 583 MPa, yield strength 702 MPa, and elongation 9%) was 281 kgf and that the simulated cladding tube had higher hardness and brittleness than the fresh zircaloy cladding tube, but the durability to abrasion was lower. To simulate the compressive stress of the spent nuclear fuel, we performed an experiment according to the size of the shale and mixing time using castable (Al_2O_3-95% + CaO-5%) and derived the fabrication requirements for producing the simulated fuel rod (stone size: 4 mm, mixing time: 10 min, sintering temperature: 900°C). Simulated ceramic fuel rods were fabricated using experimental results on the

manufacture requirements similar to spent fuel. To produce simulated fuel having mechanical properties similar to those of actual spent fuel, the mechanical decladding test was conducted by using the simulated ceramic fuel rod. The simulated ceramic fuel rod that was sintered at 800°C and 92 MPa (compressive stress) was split on one side only due to the lack of reaction force of the simulated pellet. However, the simulated ceramic fuel rod that was sintered at 900°C was split into three pieces by the mechanical decladder, with an average decladding force of approximately 235 kgf. We could then estimate that the mechanical decladder can be used for decladding of the 500-mm long PWR spent fuel rod-cuts. In the future, to manufacture the simulated spent fuel rod-cuts (Zry-4 tube + simulated pellets), simulation pellet manufacturing techniques are required, and techniques for assembling simulated pellets and simulated tubes similar to those of spent fuel rod-cuts are also necessary. If the mechanical properties of this paper are considered and the requirements of the simulated road-cut fabrication are applied, it is possible to reduce the amount of radiotoxic waste generated compared to the simulated rod-cut of oxidized decladding [7] and spent fuel. In addition, since the mechanical decladding test is performed in the nonradiation area, the mechanical decladder can be easily modified for the development of the high-throughput devices. Also, the rod-cut design requirements such as simulated cladding and simulated fuel rods can be contributed to the scaleup of mechanical decladding technology and to the simulated rod-cut manufacturing for the development of various mechanical decladding techniques.

Data Availability

The data used to support the findings of this study are available from the corresponding author upon request.

Conflicts of Interest

The authors declare that they have no conflicts of interest regarding the publication of this paper.

Acknowledgments

This work was supported by the National Research Foundation of Korea (NRF) through a grant funded by the Korea government (MEST) (no. 2012M2A8A5025696).

References

[1] K.-C. Song, H.-S. Lee, J.-M. Hur, J.-G. Kim, D.-H. Ahn, and Y.-Z. Cho, "Status of pyroprocessing technology development in Korea," *Nuclear Engineering and Technology*, vol. 42, no. 2, pp. 131–144, 2010.

[2] H. Lee, G.-I. Park, J.-W. Lee et al., "Current status of pyroprocessing development at KAERI," *Science and Technology of Nuclear Installations*, vol. 2013, Article ID 343492, 11 pages, 2013.

[3] J.-W. Lee, D.-Y. Lee, Y.-S. Lee et al., "Estimation on feeding portions of slitting decladded fuel fragments to electrolytic reduction process," *Nuclear Technology*, vol. 204, no. 1, pp. 101–109, 2018.

[4] H.-S. Lee, G.-I. Park, K.-H. Kang et al., "Pyroprocessing technology development at KAERI," *Nuclear Engineering and Technology*, vol. 43, no. 4, pp. 317–328, 2011.

[5] F. H. Hammad, H. R. Higgy, and A. A. Abdel-Rassoul, "Mechanical decladding of nuclear fuel elements," *Journal of the British Nuclear Energy Society*, vol. 10, no. 1, pp. 21–28, 1971.

[6] K. Okada, "Separation method for a spent fuel rod," European Patent Application No.: 19850302514, 1985.

[7] G. Uchiyama, K. Yamazaki, S. Sugikawa, M. Maeda, T. Tsujino, and M. Kitamur, "Development of voloxidation process for tritium control in reprocessing," *Japan Atomic Energy Research Institute-M*, vol. 23, no. 11, pp. 91–199, 1991.

[8] A. A. Abdel-Rassoul, H. R. Higgy, and F. H. Hammad, "Decladding of nuclear fuel by rolling-straightener technique," *Journal of Nuclear Energy*, vol. 23, no. 9, pp. 551–558, 1969.

[9] Y. H. Kim, Y. Z. Cho, J. W. Lee, J. H. Lee, S. C. Jeon, and D. H. Ahn, "Engineering design of a voloxidizer with a double reactor for the hull separation of spent nuclear fuel rods," *Science and Technology of Nuclear Installations*, vol. 2017, Article ID 9854830, 12 pages, 2017.

[10] Y. H. Kim, H. J. Lee, J. K. Lee et al., "Engineering design of a high-capacity vol-oxidizer for handling UO_2 pellets of tens of kilogram," *Journal of Nuclear Science and Technology*, vol. 45, no. 7, pp. 617–624, 2008.

[11] J. H. Jung, J. S. Yoon, Y. H. Kim, J. H. Jin, and D. H. Hong, "Separation and receiving device for spent nuclear fuel," United States patent No: US 7,673,544 B2, 2010.

[12] Y. H. Kim, Y. Z. Cho, Y. S. Lee, and J. M. Hur, "Engineering design of a mechanical decladder for spentnuclear rod-cuts," *Science and Technology of Nuclear Installations*, vol. 2019, Article ID 9273503, 16 pages, 2019.

[13] R. Duncan and F. CelliOe, "Nuclear reactor fuel rod splitter," United States patent No: US 3,831,248, 1974.

[14] M. Suzuki, T. Fuketa, and H. Saitou, "Analysis of pellet-clad mechanical interaction process of high-burnup PWR fuel rods by RANNS code in reactivity-initiated accident conditions," *Nuclear Technology*, vol. 155, pp. 282–292, 2017.

[15] D. S. Kim, S. B. Ahn, W. H. Oh et al., "Advanced techniques for tensile test of irradiated cladding materials," in *Proceedings of the International Symposium on Research Reactor and Neutron Science- in Commemoration of 10th Anniversary of HANARO*, Daejeon, Korea, April 2005.

[16] R. S. Daum, S. Majumdar, H. Tsai et al., "Mechanical property testing of irradiated zircaloy cladding under reactor transient conditions," in *Small Specimen Test Techniques*, vol. 4, ASTM STP 1418, West Conshohocken, PA, USA, 2002.

[17] B. K. Bae, C. H. Song, and C. S. Seok, "A Study on the mechanical properties of nuclear fuel cladding materials," *Transaction of the Korean Society of Mechanical Engineers*, vol. 27, no. 2, pp. 231–238, 2003.

[18] J. Desquines, B. Cazalis, C. Bernaudat, C. Poussard, X. Averty, and P. Yvon, "Mechanical properties of zircaloy-4 PWR fuel cladding with burnup 54-64MWd/kgU and implications for RIA behavior," *Journal of ASTM International*, vol. 2, no. 6, Article ID JAI12465, pp. 851–871, 2005.

[19] I. Scha¨ffler, P. Geyer, P. Bouffioux, and P. Delobelle, "Thermomechanical behavior and modeling between 350°C and 400°C of zircaloy-4 cladding tubes from an unirradiated state to high fluence," *Journal of Engineering Materials and Technology*, vol. 122, no. 2, pp. 168–176, 2000.

[20] D. L. Hagrman, G. A. Reyman, and R. E. Mason, "MATPRO-V.11 revision 1: a hand book of materials properties for use in

the analysis of light water reactor fuel rod behavior," NUREG/CR-0497 TREE-1280, EG & G, Gaithersburg, MD, USA, 1981.

[21] A. M. Garde, G. P. Smith, and R. C. Pirek, "Effects of hydride precipitate localization and neutron fluence on the ductility of irradiated zircaloy-4," in *Zirconium in the Nuclear Industry: Eleventh International Symposium, ASTM STP 1295*, E. R. Bradley and G. P. Sabol, Eds., pp. 407–430, American Society for Testing and Materials, West Conshohocken, PA, USA, 1996.

[22] K. H. Kang, C. H. Lee, M. K. Jeon, S. Y. Han, G. I. Park, and S.-M. Hwang, "Characterization of cladding hull wastes from used nuclear fuels," *Archives of Metallurgy and Materials*, vol. 60, no. 2, pp. 1199–1203, 2015.

[23] K. Tanaka, K. Maeda, S. Sasaki, Y. Ikusawa, and T. Abe, "Fuel—cladding chemical interaction in MOX fuel rods irradiated to high burnup in an advanced thermal reactor," *Journal of Nuclear Materials*, vol. 357, no. 1–3, pp. 58–68, 2006.

[24] J. A. King, T. J. Malewitz, S. M. James, and B. D. Simmons, "Mechanical decladding of irradiated FFTF mixed oxide fuel rods," *Transactions of the American Nuclear Society*, vol. 117, p. 333, 2017.